

Optimization of smoke exhaust efficiency under a lateral central exhaust ventilation mode in an extra-wide immersed tunnel*

Song-lin LIU, Liang WANG^{†‡}, Ming-gao YU, Yong-dong JIANG

State Key Lab of Coal Mine Disaster Dynamics and Control, Chongqing University, Chongqing 400044, China

[†]E-mail: lw38c@cqu.edu.cn

Received July 30, 2020; Revision accepted Dec. 13, 2020; Crosschecked Apr. 7, 2021

Abstract: This study focused on increasing the efficiency of the smoke exhaust system of an extra-wide (eight-lane, dual-directional) immersed tunnel with a specific quantity of exhaust. The Shenzhen–Zhongshan immersed tunnel was selected as the application example. A numerical simulation based on fire dynamics simulator was conducted. In the model, the concrete structure of the main body of the immersed tubes was not altered. The adoption of supplementary exhaust ducts increased the efficiency from 73% to 98% under the condition of no longitudinal wind. When a 50-MW fire occurred between two adjacent ducts, with a longitudinal wind velocity of 2 m/s, the efficiency reached 88% or more when the two ducts were opened. Furthermore, a safety evacuation path was developed. The results suggest that the addition of supplementary exhaust ducts combined with a rational longitudinal wind velocity is necessary for an extra-wide immersed tunnel.

Key words: Tunnel fire; Lateral central smoke exhaust; Supplementary exhaust duct; Large eddy simulation
<https://doi.org/10.1631/jzus.A2000336>

CLC number: U458.1

1 Introduction

In recent years, underwater tunnels have drawn increasing attention from researchers. This type of tunnel has many advantages. For example, they do not occupy any navigation channels and are eco-friendly (An, 2017). Thus, underwater tunnels could be a suitable alternative to traditional bridges in the infrastructure development of coastal cities.

However, tunnel fires are considered a great hazard in the operation of such tunnels. High-temperature smoke containing toxic gases generated by tunnel fires is the main cause of casualties (Vianello et al., 2012), especially when firefighters and rescuers are impeded by smoke back-layering

from downstream to upstream. The conventional method used to prevent smoke back-layering is to increase the longitudinal wind velocity. Thomas (1968) first introduced the concept of critical velocity, which is the minimum air velocity required to suppress the spread of smoke. Critical velocity is considered one of the most important parameters in tunnel fire safety. It is influenced by factors such as the fire heat release rate (HRR) and the cross-sectional geometry of tunnels, and has been investigated extensively (Oka and Atkinson, 1995; Atkinson and Wu, 1996; Wu and Bakar, 2000; Carvel et al., 2004; Hu, 2006; Xu, 2007; Hu et al., 2008; Li et al., 2010; Tanaka et al., 2018).

In addition, smoke control capability in long tunnels—especially underwater tunnels—has received considerable attention. Vauquelin and Mégret (2002) defined the efficiency of an exhaust duct as the ratio of the extracted smoke volume flow rate (VFR) to the produced VFR. After performing tests in a 1:20-scale model tunnel, Lee et al. (2010) asserted

[‡] Corresponding author

^{*} Project supported by the National Key R&D Program of China (No. 2018YFC0808103)

 ORCID: Song-lin LIU, <https://orcid.org/0000-0002-5914-2500>; Liang WANG, <https://orcid.org/0000-0001-8927-5796>

© Zhejiang University Press 2021

that smoke extraction systems play a critical role in the maintenance of visibility during a tunnel fire. Ingason and Li (2011) suggested that smoke flow from even a very large fire in a tunnel could be controlled by an appropriate extraction ventilation system. Chen et al. (2013, 2015) noted that it would be more rational and effective to combine ceiling extraction with longitudinal ventilation in the design of a tunnel ventilation system. Furthermore, they proposed a model for predicting the back-layering flow length for different distances between a ceiling extraction opening and a heat source under the combined effect of ceiling extraction and longitudinal ventilation. Critical velocity decreases with increasing smoke exhaust flow rates for a given dimensionless HRR (Tang et al., 2018). While strong longitudinal ventilation will destroy hot smoke stratification (Yang et al., 2010), a combined mode of ventilation would be more beneficial for safe evacuation.

As for an immersed tunnel, the lateral central exhaust mode is considered a rational scheme. The lateral central exhaust mode is a more specific terminological expression of central exhaust mode, primarily to distinguish it from a ceiling exhaust. In the lateral central exhaust mode, the smoke is exhausted from one side of the tunnel, not the middle of the tunnel ceiling, where the tunnel here refers to one road traffic tube, not the whole immersed tunnel tube. Examples of tunnels that employ such a scheme are the Busan-Geoje immersed tunnel in the Republic of Korea and the Hong Kong-Zhuhai-Macao bridge immersed tunnel in China (Jiang, 2018). When a pipe gallery is set up between two road traffic tubes with unidirectional traffic, the upper part of the pipe gallery is used as an independent smoke extraction duct, whereas the lower part is for electric cables and evacuation (Fig. 1). However, with a smoke exhaust efficiency of only 45.94% (Chen et al., 2017), the lateral central exhaust mode is not suitable for eight-lane, dual-directional, extra-wide immersed tunnels as it is unable to meet the requirements for safe evacuation. Significantly increasing the exhaust quantity is unfeasible because of the plug-holing effect (Mei et al., 2017).

To prevent the plug-holing effect and excessive entrainment of fresh air, supplementary exhaust ducts have been adopted. Such additional ducts hinder the flow of fire-induced smoke along the ceiling and

concurrently weaken the effect of longitudinal ventilation near the ceiling. Studies on the efficiency of smoke exhaust systems have all been based on ceiling extraction ducts (Vauquelin and Mégret, 2002; Lin and Chuah, 2008; Yang et al., 2010; Ingason and Li, 2011; Chen et al., 2013, 2015; Yi et al., 2015; Li et al., 2016; Mei et al., 2017; Tang et al., 2018) or lateral central extraction ducts (Lee et al., 2010; Chen et al., 2017; Jiang, 2018), although no obvious obstacles to the flow of smoke or fresh air exist. However, studies devoted to the blocking effect of smoke exhaust systems are scant.

To enhance understanding of smoke exhaust systems and longitudinal ventilation engineering of tunnels, it is essential to study the efficiency of modified lateral central exhaust systems combined with a rational longitudinal wind velocity. This will provide theoretical support to guide smoke control and safe evacuation. Therefore, in this study we conducted a series of simulations with a fire dynamics simulator (FDS) to investigate the effects of the mode of opening of supplementary exhaust ducts and longitudinal wind velocity. Furthermore, the efficiency of smoke exhaust was analyzed by varying the longitudinal wind velocity.

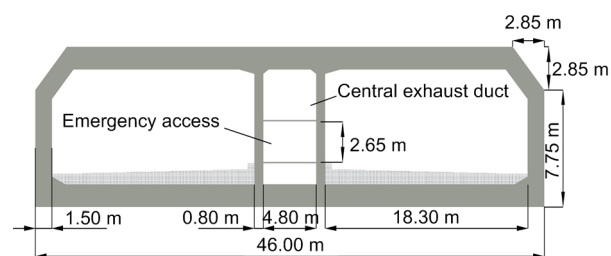


Fig. 1 Cross-sectional schematic of an eight-lane, dual-directional, immersed tunnel

2 Background

The Shenzhen–Zhongshan immersed tunnel is 6.8 km long, and is part of the Shenzhen–Zhongshan river crossing channel (Song et al., 2020). The standard cross-section of this immersed tunnel is 46 m wide and 10.6 m high with eight lanes, and the cross-section of one road traffic tube is 3.75 m wider than one of the Hong Kong-Zhuhai-Macao bridge immersed tunnels (Fig. 1). The net height of the

emergency access tunnel is 2.65 m, which is shared by two road traffic tubes. Moreover, the set interval of each fire door is 82.5 m, which is half the length of the standard tube section. The area of the central exhaust duct is more than 15 m².

To prevent a plug-holing effect and excessive entrainment of fresh air, supplementary exhaust ducts are adopted to divide the exhaust for dispersing the negative pressure (Fig. 2). Supplementary exhaust ducts, which are 18.3 m long and 7.2 m wide, can be bottom opening or side opening. There are two big dampers on each duct in the bottom opening mode and six smaller dampers in the side opening mode. The set interval of each duct is 60 m. These dampers, which are driven by electric motor, are controlled by a specific system.

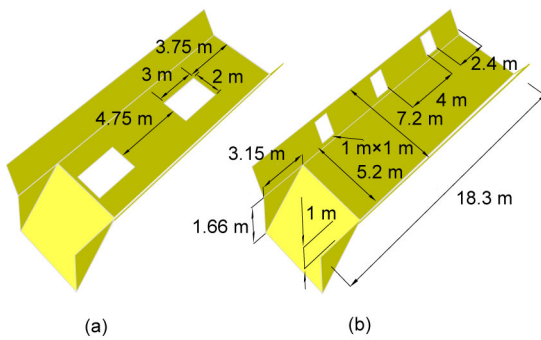


Fig. 2 Schematic of supplementary exhaust ducts
(a) Bottom opening; (b) Side opening

3 Numerical modeling

3.1 Theoretical basis

FDS (version 6) is a computational fluid dynamics (CFD) open source software package developed by the National Institute of Standards and Technology (NIST) in the USA, which has been widely adopted to simulate tunnel fires. Lee and Ryou (2006) compared the results from an experimental study and those from a numerical study using FDS, and noted that FDS can be used to predict smoke propagation in tunnel fires. Wang (2012) investigated the influence of fire scale, blockages, and ventilation rate on the propagation of smoke as well as flame length using FDS and both of its experimental models. A good agreement was achieved between the simulation and experimental results.

Relevant studies have shown that FDS is an effective and reliable numerical tool for studying tunnel fires.

FDS includes a direct numerical simulation (DNS) model and a large eddy simulation (LES) model. Both models were developed based on basic conservation laws, such as the conservation of mass, momentum, and energy combined with turbulent modeling equations. The governing conservation equations employed are as follows (Anderson et al., 1984).

Conservation of mass:

$$\frac{\partial \rho}{\partial t} + \nabla \cdot \rho \mathbf{u} = \dot{m}_b''', \quad (1)$$

where ρ is the density (kg/m³), t is the time (s), \mathbf{u} is the velocity (m/s), and \dot{m}_b''' is the mass production rate per unit volume (kg/(m³·s)).

Conservation of momentum (Newton's second law):

$$\frac{\partial}{\partial t}(\rho \mathbf{u}) + \nabla \cdot \rho \mathbf{u} \mathbf{u} + \nabla p = \rho \mathbf{g} + \mathbf{f}_b + \nabla \cdot \boldsymbol{\tau}_{ij}, \quad (2)$$

where p is the pressure (Pa), \mathbf{g} is the acceleration of gravity (m/s²), \mathbf{f}_b is the external force vector (kg/(m²·s²)), and $\boldsymbol{\tau}_{ij}$ is the viscous stress tensor (kg/(m·s²)).

Conservation of energy (the first law of thermodynamics):

$$\frac{\partial}{\partial t}(\rho h) + \nabla \cdot \rho h \mathbf{u} = \frac{Dp}{Dt} + q''' - q_b''' - \nabla \cdot \mathbf{q}'' + \varepsilon, \quad (3)$$

where h is the enthalpy (kJ/kg), q''' is the heat release rate per unit volume (kW/m³), q_b''' is the energy transferred to the evaporating droplets (kW/m³), \mathbf{q}'' is the heat flux vector (W/m²), and ε is the dissipation rate (W/m³).

Equation of state for a perfect gas:

$$p = \frac{\rho R T}{\bar{w}}, \quad (4)$$

where R is the universal gas constant (J/(mol·K)), T is the temperature (K), and \bar{w} is the molecular weight of gas mixture (kg/mol).

The LES model is derived by applying a low-pass filter of width Δ (m) to the DNS equations. In FDS, the filter width is taken to be the cube root of the cell volume, i.e. $\Delta=(V_c)^{1/3}$, and $V_c=\delta x\delta y\delta z$. Then, for any continuous field, Φ , a filtered field is defined as follows (McGrattan et al., 2013a):

$$\begin{aligned} \bar{\phi}(x, y, z, t) \\ = \frac{1}{V_c} \int_{x-\delta x/2}^{x+\delta x/2} \int_{y-\delta y/2}^{y+\delta y/2} \int_{z-\delta z/2}^{z+\delta z/2} \phi(x', y', z', t) dx' dy' dz'. \end{aligned} \quad (5)$$

The filter width Δ is closely related to the precision of the FDS simulation results. Studies on grid size sensitivity have shown that the accuracy of the model depends on the characteristic fire diameter D^* (McGrattan et al., 2013a), which is defined as

$$D^* = \left(\frac{Q}{\rho_0 C_p T_0 \sqrt{g}} \right)^{2/5}, \quad (6)$$

where Q is the heat release rate from fire (kW), ρ_0 is the density of ambient (kg/m^3), C_p is the constant pressure specific heat ($\text{kJ}/(\text{kg}\cdot\text{K})$), and T_0 is the temperature of ambient (K).

It is suggested that the cell size near the fire source should be in the range of $0.05D^*-0.1D^*$, while the larger grid size used in the far field should not exceed $0.5D^*$ (Patterson, 2002). According to the relevant requirements of the project, the fire load in the present study was set as 50 MW. For a 50-MW fire, $D^*=4.4$ m, $0.1D^*=0.44$ m, and $0.5D^*=2.2$ m.

Fig. 3 presents a schematic of the mesh near the fire. The maximum cell size was 0.25 m near the fire source and supplementary exhaust ducts, and 0.5 m in other domains. The fire source was set in the center of the model tunnel at different longitudinal positions (Fig. 4), and the effect of a traffic jam while the fire occurred was considered. To better present the actual fire situation, the area of the fire source was set to approximate the actual size. The actual size was obtained from the following equation (Karlsson and Quintiere, 1999):

$$Q = A_f \dot{m}_\infty'' (1 - e^{-k_p D}) \chi \Delta H_c, \quad (7)$$

where A_f is the horizontal burning area of fuel (m^2), \dot{m}_∞'' is the fuel burning rate for a large diameter ($\text{kg}/(\text{s}\cdot\text{m}^2)$), k_p is the material constant for liquid fuels (m^{-1}), D is the diameter (m), χ is the combustion efficiency (%), and ΔH_c is the complete heat of combustion (kJ/kg).

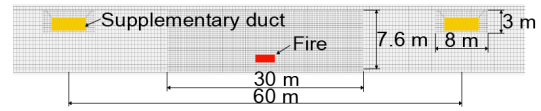


Fig. 3 Schematic of the mesh near the fire

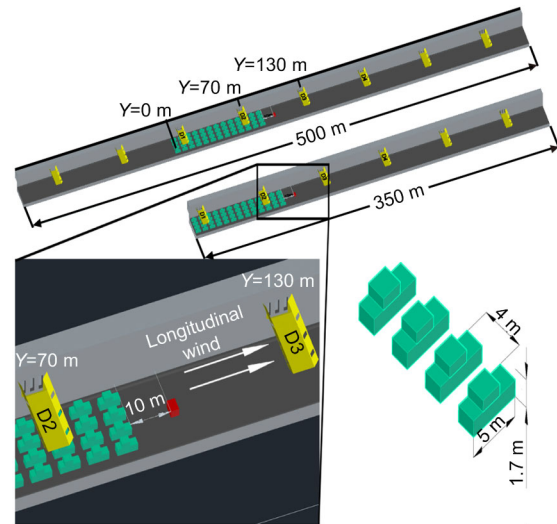
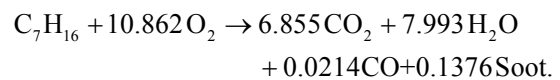


Fig. 4 Schematic of the overall view

Y represents the location in the longitudinal direction; D_i is the serial number of the i th duct

The calculated fire area was 15.96 m^2 , so the fire source was set to $4 \text{ m} \times 4 \text{ m}$ and the fire source surface was 1 m above the ground. Regardless of the growth and decay phase of the fire, only the steady phase was considered. The HRR was set to 50 MW to consider the worst case condition.

Heptane (C_7H_{16}) was chosen as the reaction type, where $\text{CO_YIELD}=0.006$, $\text{SOOT_YIELD}=0.015$, and the hydrogen fraction is 0.1. The default reaction equation was defined as



The energy release per unit mass oxygen is $13100 \text{ kJ}/\text{kg}$, and thus the quantity of soot produced

per second in a 50-MW fire can be calculated as 16.47 g/s. The ratio between the quantity of soot extracted and the quantity of soot produced is termed the efficiency of the smoke exhaust, and is given as follows (Chen et al., 2017):

$$\eta = \frac{m_e}{m_p} \times 100\%, \quad (8)$$

where η is the efficiency of smoke exhaust (%), m_e is the extracted soot quantity (g/s), and m_p is the produced soot quantity (g/s).

3.2 Case introduction

Studies on the efficiency of smoke exhaust systems have all been based on ceiling extraction ducts or lateral central extraction ducts, with no obvious obstacle to the flow of smoke or fresh air. However, a blocking effect will cause the accumulation of smoke between two supplementary exhaust ducts; therefore, opening more than two ducts is not recommended. Through establishing two area statistics to monitor the mass flux of soot in the two ducts (Fig. 5), it is easy to obtain these specific data in a numerical study.

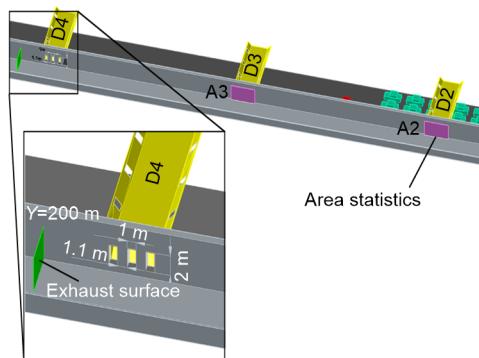


Fig. 5 Schematic of the exhaust surface and area statistics
 A_i is the area statistic of the corresponding duct D_i

Different opening modes might have an impact on the efficiency of smoke exhaust. To compare two types of opening mode of supplementary exhaust ducts—namely bottom openings and side openings, corresponding to the vertical direction and longitudinal direction, respectively—three cases were examined in this study: bottom openings, side openings, and the absence of supplementary ducts. These three cases were modeled over 600 s for a 500-m length of

model. Other cases were established to ascertain the effect of longitudinal wind velocity on the smoke exhaust efficiency. Each case was modeled over 300 s for a 350-m length of model, as summarized in Table 1. The maximum longitudinal wind velocity (3.2 m/s) in the cases was slightly lower than the critical velocity (3.44 m/s) of this immersed tunnel, which was calculated using the formula of Wu and Bakar (2000) without considering the effect of smoke exhaust. Because the critical velocity decreases with increasing smoke exhaust flow rates for a given dimensionless HRR (Tang et al., 2018), it is rational to reduce the computational load.

The ambient temperature was set as 20 °C and the pressure as 101 kPa. The construction material of the tunnel was specified as “CONCRETE,” and its density, specific heat, and conductivity were set as 2280.0 kg/m³, 1.04 kJ/(kg·K), and 1.8 W/(m·K), respectively. The volume flow of the exhaust surface was 250 m³/s, the same as the value of the Hong Kong-Zhuhai-Macao bridge (Jiang, 2018); the activation time of the 50-MW fire was $t=0$ s, and the start-up time of the smoke exhaust system was $t=20$ s.

4 Results and discussion

To verify the effectiveness of supplementary exhaust ducts, it would be rational to take the total quantity of soot extracted as the main criterion. Adding the quantity of soot extracted estimated by the two area statistics (A2 and A3 in Fig. 5) until the value becomes steady, the efficiency can be calculated using Eq. (7). Because this represents a change from traditional disposal methods in dealing with smoke during tunnel fires, it is essential to confirm the security of evacuation under the adoption of supplementary ducts.

4.1 Comparison of different opening modes

As shown in Fig. 6 (p.402), the mean values of extracted soot quantities during the stable stage under the different types of opening modes from large to small were 16.18 g/s, 14.02 g/s, and 12.06 g/s, which corresponded to side openings, bottom openings, and no supplementary ducts, respectively. Furthermore, a peak value was observed in the curves of the two opening modes. These two curves became steady

earlier than the curve for the absence of supplementary ducts. This demonstrated that the blocking effect of supplementary ducts caused the accumulation of smoke, which could increase the smoke exhaust efficiency by up to 98%. Moreover, the efficiency of the side opening was 13.2% higher than that of the bottom opening, as a result of the longitudinal flow of smoke. Notably, the efficiency of no ducts was

73.2%. However, this does not suggest that the efficiency (45.94%) of the same immersed tunnel model obtained by Chen et al. (2017) was wrong, because the volume flow of the exhaust surface in the present study was 61 m^3 higher.

Fig. 7 shows the top view of the smoke flow with different types of opening modes when $t=500 \text{ s}$. The case of the side opening was clearly better able to

Table 1 Description of different fire scenarios

Case No.	Location of the fire, Y (m)	Supplementary ducts opened	Length of the model (m)	Longitudinal wind velocity (m/s)	Total cells
1	100	D2, D3 (side)	500	0.0	994 560
2		D2, D3 (bottom)		0.0	
3		Absence of ducts		0.0	
4	65	D2, D3 (side)	350	1.8	775 680
5				2.0	
6				2.4	
7				2.8	
8				3.2	
9	70	D2, D3 (side)	350	1.8	775 680
10				2.0	
11				2.4	
12				2.8	
13				3.2	
14	85	D2, D3 (side)	350	1.8	811 520
15				2.0	
16				2.4	
17				2.8	
18				3.2	
19	100	D2, D3 (side)	350	1.8	802 560
20				2.0	
21				2.4	
22				2.8	
23				3.2	
24	115	D2, D3 (side)	350	1.8	811 520
25				2.0	
26				2.4	
27				2.8	
28				3.2	
29	125	D2, D3 (side)	350	1.8	775 680
30				2.0	
31				2.4	
32				2.8	
33				3.2	
34	130	D2, D3 (side)	350	1.8	775 680
35				2.0	
36				2.4	
37				2.8	
38				3.2	

contain the spread of smoke. Even without longitudinal wind velocity, the length of smoke back-layering downstream was shorter than that upstream because of the shorter distance from the exhaust surface. The D3 duct extracted more smoke than did the D2 duct.

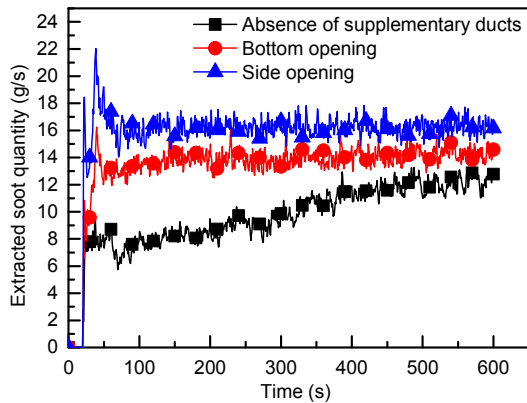


Fig. 6 Extracted soot quantity with different opening modes and without longitudinal wind

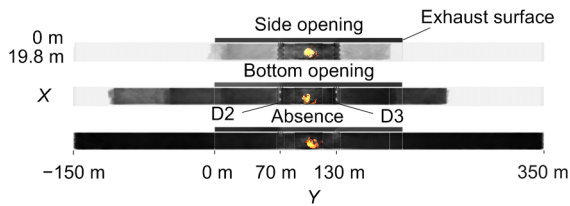


Fig. 7 Top view of smoke flow with different opening modes and without longitudinal wind ($t=500$ s)

4.2 Influence of longitudinal wind velocity

Fig. 8 shows the efficiency of the exhaust system with side openings in different locations with various longitudinal wind velocities, corresponding to cases 4–38. The efficiency generally decreased with fire locations from D2 to D3 (Fig. 8a). When the wind velocity was small (1.8 or 2.0 m/s), as the distance of the fire from D2 ($Y=70$ m) increased, the efficiency showed a linear downward trend and declined sharply after $Y=125$ m. This showed that under a lower wind velocity, the main factor affecting the efficiency was the distance of the fire from D2. The greater the distance, the greater the amount of fresh air that was extracted by D2. This suggests that regulating the dampers of D2 and D3 in different flow volumes could be beneficial for increasing the efficiency. When the fire location was further than $Y=125$ m, the

smoke was divided into two parts by duct D3 because of a deviation of the fire plume caused by longitudinal wind. Only part of the smoke was gathered between D2 and D3 before being extracted by these ducts. The other part of the smoke flowed easily downstream under duct D3. This was the reason for the downward trend obviously increasing after $Y=125$ m. Moreover, when the longitudinal wind velocity was high (2.4, 2.8, or 3.2 m/s), the relationship between the efficiency and distance of the fire location from D2 was nonlinear. This showed that the main factor affecting the efficiency became wind velocity (Fig. 8b). Except for the two curves of fire location at $Y=125$ m and $Y=130$ m in Fig. 8b, the rate of decline of efficiency of other curves increased with the wind velocity, which means that the effect of wind velocity was nonlinear. Higher wind velocities hindered the stratification of hot smoke, causing more fresh air to be extracted by the exhaust system. As for the other two curves

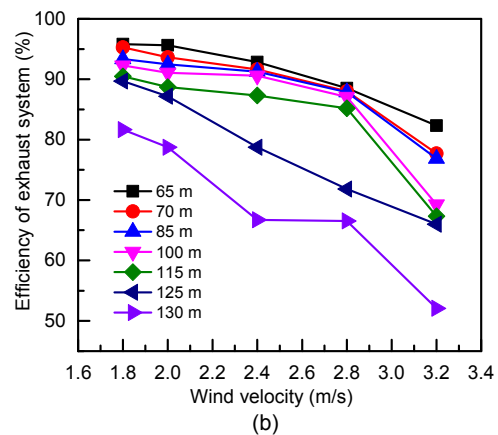
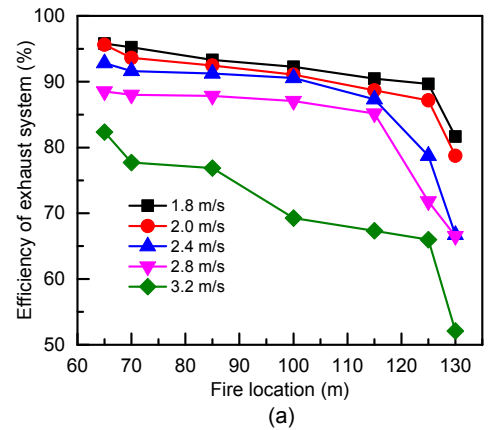


Fig. 8 Efficiency of the exhaust system at different locations with various longitudinal wind velocities (a) Fire location; (b) Wind velocity

($Y=125$ m and $Y=130$ m) in Fig. 8b, because the ducts did not work well in accumulating smoke, higher wind velocities exacerbated this phenomenon.

4.3 Evacuation path development

For the safe evacuation of people from the tunnel, the air in the evacuation path is required to be clear of smoke to a height of at least 2.0 m. In modeling methods, a height of at least 2.5 m must be maintained above the evacuation path for the reason of precision (NASEM, 2011). Figs. 9–15 present the temperature profiles in the middle of the tunnel ($X=$

10 m) under a steady state where the temperature of the grey area is below 40 °C, and the solid line is 2.5 m above the evacuation path. The maximum exposure time without incapacitation at 40 °C is

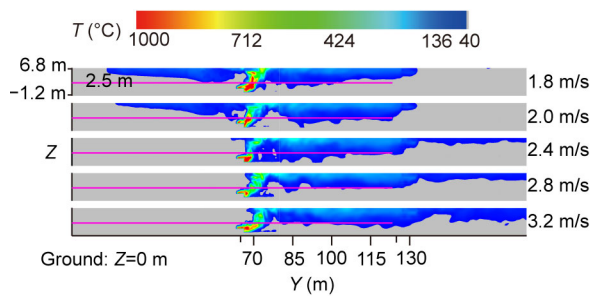


Fig. 9 Temperature profiles when the center of the fire is located at $Y=65$ m. References to color refer to the online version of this figure

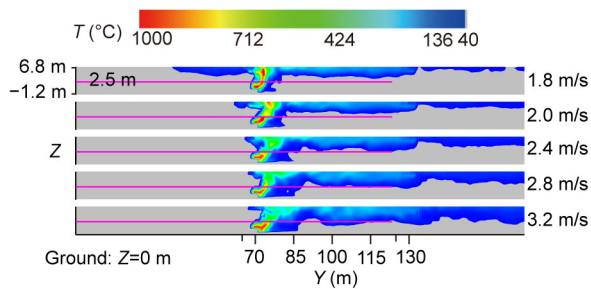


Fig. 10 Temperature profiles when the center of the fire is located at $Y=70$ m

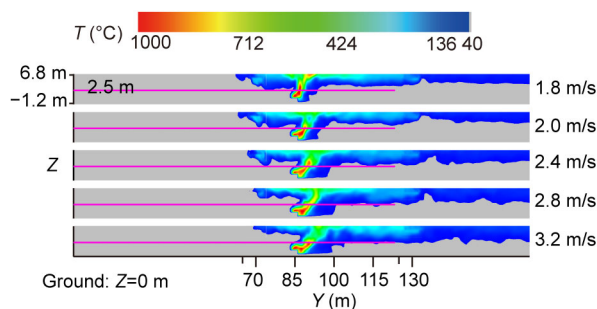


Fig. 11 Temperature profiles when the center of the fire is located at $Y=85$ m

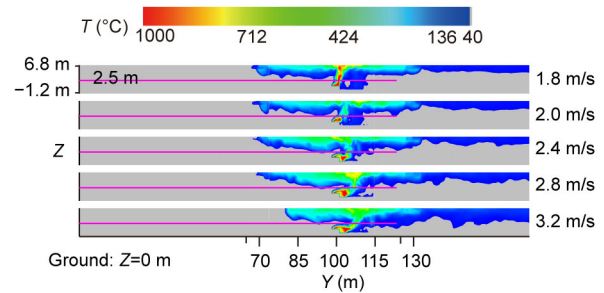


Fig. 12 Temperature profiles when the center of the fire is located at $Y=100$ m

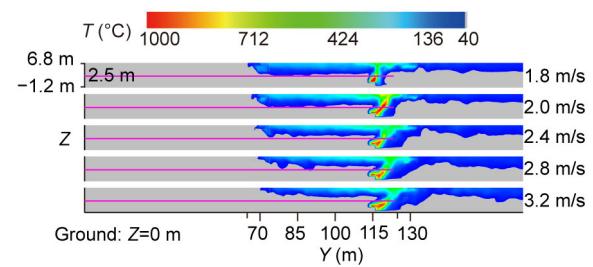


Fig. 13 Temperature profiles when the center of the fire is located at $Y=115$ m

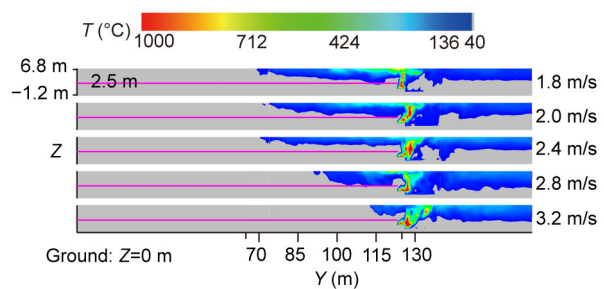


Fig. 14 Temperature profiles when the center of the fire is located at $Y=125$ m

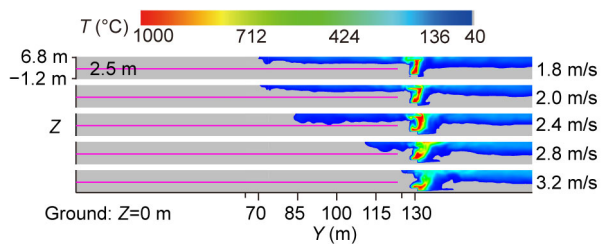


Fig. 15 Temperature profiles when the center of the fire is located at $Y=130$ m

40.2 min (NASEM, 2011), which is enough for safe evacuation. Notably the application of tenability criteria at the perimeter of a fire is impractical. The zone of tenability must be defined to apply outside a boundary away from the perimeter of the fire, which depends on the HRR and radiation, and could be as much as 30 m (NASEM, 2011). Therefore, the boundary of the evacuation path that should be considered is about 15 m upstream from the center of the fire. Apparently, every case shown in Figs. 9–15 would satisfy this criterion. In addition, as for cases 4, 5, and 9 (corresponding to 1.8 and 2.0 m/s in Fig. 9 and 1.8 m/s in Fig. 10, respectively), smoke continued to flow upstream after being extracted by D2, and was not controlled well between D2 and D3. This shows that opening the adjacent two ducts and providing an appropriate wind velocity was essential.

Moreover, as shown in Figs. 14 and 15, when the longitudinal wind velocity was 2.4, 2.8, or 3.2 m/s, the plume from the fires located at $Y=125$ m and $Y=130$ m did not reach the other duct (D2); no smoke was extracted by D2. In addition, the length of the smoke back-layering flow decreased with the increase of wind velocity. This showed that an excessively high wind velocity greatly suppressed smoke back-layering flow, which further explains the reduction in efficiency.

Fig. 16 illustrates the profiles of soot in the middle of the tunnel with a 2-m/s longitudinal wind velocity and at various fire locations. For 8 h at work, 9 ppm (4 mg/m^3) is the permissible concentration-time weighted average (PC-TWA) (MOH, 2007). Although there was back-layering in all situations to some extent, a tenable environment was still available for safe evacuation.

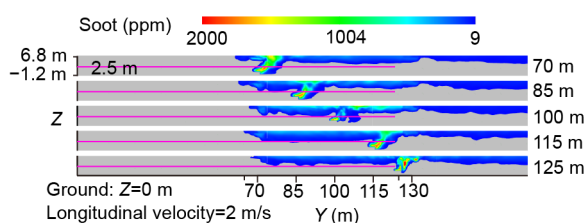


Fig. 16 Soot profiles with a 2-m/s longitudinal wind velocity at different fire locations

When considering visibility in an evacuation, smoke obscuration levels need to be continuously

maintained below the point at which a sign internally illuminated at 80 lx is discernible at 30 m, and doors and walls are discernible at 10 m (NASEM, 2011). The visibility distance V (m) can be estimated using the extinction coefficient K (m^{-1}) of the air smoke mix:

$$V = \frac{A}{K}, \quad (9)$$

where A is a constant between 2 and 6 depending on the signs to be seen (reflecting or illuminated). The default value of A in FDS is 3 (McGrattan et al., 2013b). Fig. 17 illustrates the horizontal profiles of visibility at a height of 2 m from the ground with a 2-m/s longitudinal wind velocity and at various fire locations. The red area indicates the location where the visibility is greater than 30 m, implying no visual obscuration at all. When the fire location was at $Y=115$ m or $Y=125$ m, yellow areas appeared upstream of the fire source, indicating visibility between 30 and 20 m. Even if we let the value of A change from 3 to 2 (reflecting) to convert the visibility distance, the result is still greater than 10 m. If A is 6 (illuminated), then the visibility in these areas will be much greater than 30 m. This indicates that the visibility of the yellow area is also consistent with a safe escape.

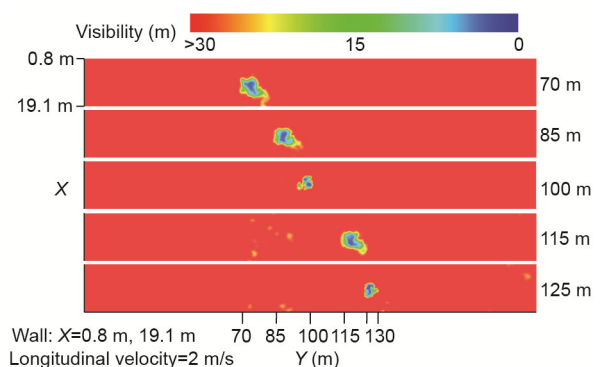


Fig. 17 Horizontal profiles of visibility with a 2-m/s longitudinal wind velocity at different fire locations. References to color refer to the online version of this figure

Overall, this smoke extraction system guarantees that the temperature, concentration of toxic substances, and visibility needed for escape are within safe limits. Note that a 1.8-m/s or even lower wind

velocity would be fine with a fire located at $Y=85$, 100, 115, or 125 m. For other fire scenarios, there would be other optimal combinations of wind velocities and exhaust systems.

5 Conclusions

In this study, a numerical investigation of smoke control during a fire in an extra-wide immersed tunnel was conducted using FDS. The effects of different opening modes of supplementary exhaust ducts on smoke control were analyzed, as were the effects of various longitudinal wind velocities. Several conclusions were drawn, as follows:

1. The addition of supplementary exhaust ducts increased exhaust efficiency from 73% to 98% under the lateral central exhaust mode without longitudinal wind.

2. The efficiency of side openings was 13.2% higher than that of bottom openings.

3. To increase the efficiency of an exhaust system, using a lower longitudinal wind velocity and the blockage of supplementary exhaust ducts offers a new approach in the design of tunnel ventilation systems for extra-wide immersed tunnels. When a 50-MW fire occurred between two ducts, by regulating the longitudinal wind velocity at 2 m/s and opening the two adjacent ducts, the efficiency could reach 88% or more. Additionally, a safety evacuation path was ensured. For an extra-wide immersed tunnel, the addition of supplementary exhaust ducts combined with a rational longitudinal wind velocity is necessary.

Notably, for smaller HRRs of fire in extra-wide immersed tunnels, more work is needed to determine a rational longitudinal wind velocity. Future studies should investigate the appropriate adjustment of dampers of supplementary exhaust ducts under different fire conditions.

Contributors

Liang WANG designed the research. Ming-gao YU processed the corresponding data. Song-lin LIU wrote the first draft of the manuscript. Yong-dong JIANG helped to organize the manuscript. Song-lin LIU revised and edited the final version.

Conflict of interest

Song-lin LIU, Liang WANG, Ming-gao YU, and Yong-dong JIANG declare that they have no conflict of interest.

References

- An GF, 2017. Technical Guide for Construction of Immersed Tunnel. China Architecture & Building Press, Beijing, China (in Chinese).
- Anderson DA, Tannehill JC, Pletcher RH, 1984. Computational Fluid Mechanics and Heat Transfer. McGraw-Hill, New York, USA.
- Atkinson GT, Wu Y, 1996. Smoke control in sloping tunnels. *Fire Safety Journal*, 27(4):335-341. [https://doi.org/10.1016/S0379-7112\(96\)00061-6](https://doi.org/10.1016/S0379-7112(96)00061-6)
- Carvel RO, Beard AN, Jowitt PW, et al., 2004. The influence of tunnel geometry and ventilation on the heat release rate of a fire. *Fire Technology*, 40(1):5-26. <https://doi.org/10.1023/B:FIRE.0000003313.97677.c5>
- Chen JZ, Cao ZM, Zhang Q, 2017. Study on the efficiency of smoke exhausting under lateral exhaust mode in extra-wide immersed tunnel fire. *Chinese Journal of Underground Space and Engineering*, 13(S1):393-399 (in Chinese).
- Chen LF, Hu LH, Tang W, et al., 2013. Studies on buoyancy driven two-directional smoke flow layering length with combination of point extraction and longitudinal ventilation in tunnel fires. *Fire Safety Journal*, 59:94-101. <https://doi.org/10.1016/j.firesaf.2013.04.003>
- Chen LF, Hu LH, Zhang XL, et al., 2015. Thermal buoyant smoke back-layering flow length in a longitudinal ventilated tunnel with ceiling extraction at difference distance from heat source. *Applied Thermal Engineering*, 78:129-135. <https://doi.org/10.1016/j.applthermaleng.2014.12.034>
- Hu LH, 2006. Studies on Thermal Physics of Smoke Movement in Tunnel Fires. PhD Thesis, University of Science and Technology of China, Hefei, China (in Chinese). <https://doi.org/10.7666/d.y919023>
- Hu LH, Peng W, Huo R, 2008. Critical wind velocity for arresting upwind gas and smoke dispersion induced by near-wall fire in a road tunnel. *Journal of Hazardous Materials*, 150(1):68-75. <https://doi.org/10.1016/j.jhazmat.2007.04.094>
- Ingason H, Li YZ, 2011. Model scale tunnel fire tests with point extraction ventilation. *Journal of Fire Protection Engineering*, 21(1):5-36. <https://doi.org/10.1177/1042391510394242>
- Jiang SP, 2018. Key Technology of Disaster Prevention and Mitigation for Offshore Extra-long Immersed Tunnels. China Communications Press, Beijing, China (in Chinese).
- Karlsson B, Quintiere JQ, 1999. Enclosure Fire Dynamics. CRC Press, Boca Raton, USA.
- Lee EJ, Oh CB, Oh KC, et al., 2010. Performance of the smoke extraction system for fires in the Busan-Geoje immersed tunnel. *Tunnelling and Underground Space Technology*, 25(5):600-606. <https://doi.org/10.1016/j.tust.2010.04.005>
- Lee SR, Ryou HS, 2006. A numerical study on smoke movement in longitudinal ventilation tunnel fires for

- different aspect ratio. *Building and Environment*, 41(6): 719-725.
<https://doi.org/10.1016/j.buildenv.2005.03.010>
- Li LJ, Tang F, Dong MS, et al., 2016. Effect of ceiling extraction system on the smoke thermal stratification in the longitudinal ventilation tunnel. *Applied Thermal Engineering*, 109:312-317.
<https://doi.org/10.1016/j.applthermaleng.2016.08.071>
- Li YZ, Lei B, Ingason H, 2010. Study of critical velocity and backlayering length in longitudinally ventilated tunnel fires. *Fire Safety Journal*, 45(6-8):361-370.
<https://doi.org/10.1016/j.firesaf.2010.07.003>
- Lin CJ, Chuah YK, 2008. A study on long tunnel smoke extraction strategies by numerical simulation. *Tunnelling and Underground Space Technology*, 23(5):522-530.
<https://doi.org/10.1016/j.tust.2007.09.003>
- McGrattan K, Hostikka S, McDermott R, et al., 2013a. Fire Dynamics Simulator Technical Reference Guide. Volume 1: Mathematical Model. NIST Special Publication 1018, National Institute of Standards and Technology, Washington, USA.
- McGrattan K, McDermott R, Weinschenk C, et al., 2013b. Fire Dynamics Simulator: User's Guide. NIST Special Publication 1019, National Institute of Standards and Technology, Washington, USA.
- Mei FZ, Tang F, Ling X, et al., 2017. Evolution characteristics of fire smoke layer thickness in a mechanical ventilation tunnel with multiple point extraction. *Applied Thermal Engineering*, 111:248-256.
<https://doi.org/10.1016/j.applthermaleng.2016.09.064>
- MOH (Ministry of Health of the People's Republic of China), 2007. Occupational Exposure Limits for Hazardous Agents in the Workplace. Part 1: Chemical Hazardous Agents, GBZ 2.1-2007. MOH, Beijing, China (in Chinese).
- NASEM (National Academies of Sciences, Engineering, and Medicine), 2011. Design Fires in Road Tunnels. The National Academies Press, Washington, USA, p.17-19.
<https://doi.org/10.17226/14562>
- Oka Y, Atkinson GT, 1995. Control of smoke flow in tunnel fires. *Fire Safety Journal*, 25(4):305-322.
[https://doi.org/10.1016/0379-7112\(96\)00007-0](https://doi.org/10.1016/0379-7112(96)00007-0)
- Patterson NM, 2002. Assessing the Feasibility of Reducing the Grid Resolution in FDS Field Modelling. Fire Engineering Research Report 02/12, University of Canterbury, Christchurch, New Zealand.
<https://doi.org/10.26021/2276>
- Song SY, Guo J, Su QK, et al., 2020. Technical challenges in the construction of bridge-tunnel sea-crossing projects in China. *Journal of Zhejiang University-SCIENCE A (Applied Physics & Engineering)*, 21(7):509-513.
<https://doi.org/10.1631/jzus.A20CSBE1>
- Tanaka F, Takezawa K, Hashimoto Y, et al., 2018. Critical velocity and backlayering distance in tunnel fires with longitudinal ventilation taking thermal properties of wall materials into consideration. *Tunnelling and Underground Space Technology*, 75:36-42.
<https://doi.org/10.1016/j.tust.2017.12.020>
- Tang F, He Q, Mei FZ, et al., 2018. Effect of ceiling centralized mechanical smoke exhaust on the critical velocity that inhibits the reverse flow of thermal plume in a longitudinal ventilated tunnel. *Tunnelling and Underground Space Technology*, 82:191-198.
<https://doi.org/10.1016/j.tust.2018.08.039>
- Thomas PH, 1968. The movement of smoke in horizontal passages against air flow. *Fire Research Technical Paper*, 7(1):1-8.
- Vauquelin O, Mégret O, 2002. Smoke extraction experiments in case of fire in a tunnel. *Fire Safety Journal*, 37(5):525-533.
[https://doi.org/10.1016/S0379-7112\(02\)00014-0](https://doi.org/10.1016/S0379-7112(02)00014-0)
- Vianello C, Fabiano B, Palazzi E, et al., 2012. Experimental study on thermal and toxic hazards connected to fire scenarios in road tunnels. *Journal of Loss Prevention in the Process Industries*, 25(4):718-729.
<https://doi.org/10.1016/j.jlp.2012.04.002>
- Wang HY, 2012. Numerical and theoretical evaluations of the propagation of smoke and fire in a full-scale tunnel. *Fire Safety Journal*, 49:10-21.
<https://doi.org/10.1016/j.firesaf.2011.12.012>
- Wu Y, Bakar MZA, 2000. Control of smoke flow in tunnel fires using longitudinal ventilation systems—a study of the critical velocity. *Fire Safety Journal*, 35(4):363-390.
[https://doi.org/10.1016/S0379-7112\(00\)00031-X](https://doi.org/10.1016/S0379-7112(00)00031-X)
- Xu L, 2007. Theoretical Analysis and Experimental Study on Smoke Control in Long Highway Tunnels. PhD Thesis, Tongji University, Shanghai, China (in Chinese).
- Yang D, Hu LH, Huo R, et al., 2010. Experimental study on buoyant flow stratification induced by a fire in a horizontal channel. *Applied Thermal Engineering*, 30(8-9): 872-878.
<https://doi.org/10.1016/j.applthermaleng.2009.12.019>
- Yi L, Wei R, Peng JZ, et al., 2015. Experimental study on heat exhaust coefficient of transversal smoke extraction system in tunnel under fire. *Tunnelling and Underground Space Technology*, 49:268-278.
<https://doi.org/10.1016/j.tust.2015.05.002>